ELECTRONIC TRANSPORT IN AMORPHOUS CARBON

J. P. SULLIVAN, T. A. FRIEDMANN
Sandia National Laboratories, MS 1421, Albuquerque, NM 87185-1421, USA
E-mail: jpsulli@sandia.gov

Electronic transport in a-C films has been the subject of considerable debate. In this study, combined stress relaxation and electrical transport studies were used to identify the transport mechanism in a-C films prepared by pulsed-laser deposition. The stress relaxation was modeled by a first-order kinetic reaction involving transformation of 4-fold coordinated carbon atoms to 3-fold coordinated carbon atoms, and the distribution of activation energies for this process was determined. The activation energies were found to range from about 1 eV to over 2 eV, and using these activation energies, the increase in 3-fold carbon concentration with time-temperature annealing was obtained Conductivity measurements were also performed as a function of time-temperature annealing. It was found that the conductivity of a-C films is exponentially proportional to increases in 3-fold carbon concentration. This result can be explained by thermally activated hopping along carbon 3-fold chains combined with chain-to-chain tunneling. From the data, a typical chain length was estimated to consist of 13 carbon atoms. The heterogeneous nature of the conductivity may explain the spatially localized electron emission which is observed in a-C assuming a tunnel barrier emission model.

1 Background

1.1 Introduction

Amorphous carbon, a-C, is an interesting material which exhibits unique and technologically important electronic properties, particularly in the area of field emission [1]. In this article, we review some of the current understanding of the electronic properties of this material, and then present new results on the identification of the electronic transport mechanism using combined stress relaxation and electrical conductivity measurements. For purposes of this article, a-C specifically refers to hydrogen-free, resistive films of carbon containing a majority of sp^3 bonding. Because of ambiguities in defining local bond hybridization, descriptions based on sp^3 and sp^2 will be avoided in the remainder of the text in favor of descriptions based on the local coordination of the carbon atom, viz. 4-fold and 3-fold coordination.

The electron transport mechanism and doping of a-C have been debated for many years. With the advent of a number of recent *ab initio* structure calculations, there is now general agreement regarding the electronic structure of this material [2]. The integrated density of states, DOS, reveals an approximate 2 to 3 eV band gap, but the band structure differs in detail from other more conventional amorphous

DISCLAIMER

semiconductors, e.g. a-Si and a-Ge. The most apparent difference is that the deepest lying states in a-C (the states most responsible for defining the band edges) have π and π^* symmetry which is associated with a large (~ 30%) concentration of 3-fold coordinated carbon atoms. In contrast, 3-fold coordination is absent, except in isolated defect structures, for a-Si and a-Ge. Theory also indicates that the 3-fold atoms in a-C are not uniformly distributed within the matrix of 4-fold coordinated atoms, but rather there is a tendency for the 3-fold atoms to link up as extended conjugated chain-like structures. The degree of segregation and the possible spatial extent of these structures are not readily determined from calculations due to limitations on practical unit cell size.

1.2 Doping in a-C

There has been considerable debate concerning the transport mechanism of a-C and, in particular, the doping of a-C. Most of the earlier work focused on doping in hydrogenated analogs of a-C, a-C:H, due principally to the fact that highly insulating hydrogen-free a-C films have only been available recently. In one of the earlier works in this field, Meyerson and Smith [3,4] examined B and P-doped a-C:H films and concluded that B and P were acting like true p- and n-type dopants – B incorporation moving E_F down into the valence band (VB) tail states and P incorporation moving E_F up into the conduction band (CB) tail states. Their conclusions were based, in part, on observations that the activation energy for transport decreased and the conductivity increased when both B and P were incorporated. Jones and Stewart [5] also examined B and P-doped, as well as N-doped, a-C:H films and instead concluded that the observed enhancement in conductivity was not due to movement of E_F towards either the CB or VB tail states, but rather was due to an increase in the density of states near E_F, i.e. not a true doping effect. Almost all work since that time has either supported one or the other of these opposing views.

Amir and Kalish [6], Stenzel *et al.* [7], Ronning *et al.* [8], and Helmbold *et al.* [9] concluded that incorporation of dopants, specifically P or N, into a-C:H or a-C does not give rise to a true doping effect, but instead results in modification of the DOS near E_F or the band edges. In contrast, Veerasamy *et al.* [10], Amaratunga *et al.* [11], and Silva *et al.* [12] concluded that dopants, specifically N, can give rise to a true doping effect in which E_F is moved upwards toward CB tail states.

Because the role of N doping in a-C has been the focus of much of the experimental work, it is useful to look carefully at the experimental evidence to date. There is one important point regarding N doping that is concluded by almost

all researchers in the field: at high N concentrations, N increases the concentration of 3-fold coordinated carbon which results in an increase in the conductivity of the a-C film by increasing the DOS near E_F (or in the band tails) or by increasing the connectivity between 3-fold sites. This microstructural effect of N has been confirmed by optical absorption and/or EELS measurements [6,7,10,12] and by ultraviolet photoelectron spectroscopy (UPS) [13]. The issue of more significance is the role of N at dilute concentrations. Veerasamy *et al.* concluded that N acts as an electronic dopant up to a threshold concentration of about 1 at. % for a-C [10], while Silva *et al.* concluded that the threshold was at about 7 at. % for a-C:H [12].

Two of the main experimental arguments for N acting as an n-type dopant are centered on measured changes in the activation energy for electrical transport and changes in electrical conductivity. Instead of a monotonic decrease in activation energy and monotonic increase in conductivity, Veerasamy *et al.* and Silva *et al.* observed that the activation energy first increased (with a corresponding decrease in electrical conductivity) up to a critical N concentration which is below the threshold concentration [10,12]. These authors explained the effect as follows: undoped a-C(:H) is intrinsically p-type with E_F lying below mid-gap near VB tail states. At low N concentrations, N incorporation acts as an electron donor and first compensates the acceptor states, causing E_F to move through mid-gap towards CB tail states. The maximum in E_A would then be found for the fully compensated material and would roughly correspond to 1/2 of the mobility gap of a-C(:H), which is approximately 2 eV.

Not all groups observe this conductivity decrease followed by a conductivity increase for low N concentrations. Ronning *et al.* observed a monotonic increase in conductivity with N incorporation for a-C films over the same concentration range that Veerasamy *et al.* observed a conductivity minimum [8]. In addition, Amir and Kalish [6] and Helmbold *et al.* [9] observed monotonic increases in conductivity with increasing N content in a-C:H films over the same concentration range in which Silva *et al.* [12] observed a conductivity minimum. At minimum, it can be concluded that the effect of N in a-C or a-C:H films must be strongly dependent on precise details of how the film was synthesized.

There are several problems with using measurements of electrical conductivity and activation energy to assess electronic doping in a-C. The first problem is that it is typically observed that the conductivity increases and activation energy decreases when simply the 3-fold content of a-C films increase [5]. These changes are believed to be due to decreases in the mobility gap (essentially the π - π^* gap) as the concentration of 3-fold sites and, hence, the sizes of the connected 3-fold regions increase. A second problem with conductivity measurements is that

Arrhenius plots of conductivity versus temperature are frequently non-linear which makes identification of an activation energy for transport ambiguous [9,12]. This problem is further complicated by the fact that it is necessary to limit the temperature of electrical measurement to less than 200°C and probably even less than 100°C for hydrogen and nitrogen containing a-C films. Irreversible changes in conductivity occur above these temperatures [14]. Finally, it is necessary to limit the voltage applied to the a-C film when measuring the current-voltage characteristics because the conduction behavior is ohmic only for applied fields less than about 10^4 V/cm and irreversible changes in the film occur for fields in excess of about 2×10^5 V/cm [8]. Because of these difficulties, it would be desirable to have independent measurement of the ability of N to act as an n-type dopant which is not dependent on changes in conductivity or activation energy.

The measurement of thermopower, S, is one such measurement. Several measurements of the thermopower of P or N containing a-C:H films have been performed [4,6,9], but the interpretation has not been straightforward. The measurement of thermopower is hampered by the high resistivities and low mobilities of the films, and hence measurement of the most resistive films (i.e. undoped or very lightly doped films) is less reliable. Of the measurements which are considered reliable, all workers observe low thermopowers, in the μV/K range, which is consistent with carrier conduction by hopping transport. Furthermore, the slope of a plot of S versus 1/T is typically much lower than the measured activation energy for electrical conduction, which further suggests the absence of extended state conduction in these materials [15]. The sign of the thermopower is related to the slope of the DOS near E_F, and for conventional semiconductors negative thermopowers imply conduction by electrons and positive thermopowers imply conduction by holes. For doped a-C:H the behavior is not clear. Meyerson and Smith observed small negative thermopowers for P containing a-C:H films and small positive thermopowers for B containing films [4]. Amir and Kalish observed both negative and positive thermopowers for N-containing a-C:H films, the negative values being observed for films containing N concentrations between 1.8 and 6.8 at. % with positive values being observed for films of higher and lower N concentrations [6]. Helmbold *et al.* observed negative thermopowers for both undoped and P containing a-C:H films [9]. No firm conclusion can be drawn from thermopower measurements regarding the role of N and P as electronic dopants except that the conduction process is dominated by hopping.

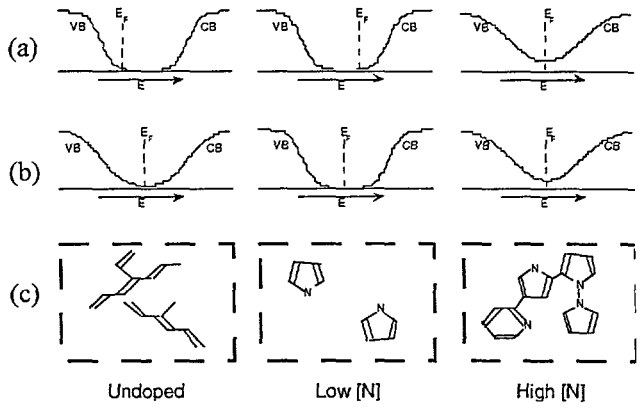

Figure 1: (a) Schematic DOS for electronic doping by N in a-C for three doping levels: undoped, lightly doped, and heavily doped. (b) Schematic DOS for microstructural doping by N. (c) Schematic structural models for microstructural doping by N.

If N is *not* acting as a true electronic dopant, how can its influence on the electronic properties of a-C(:H) be explained, particularly at the low doping concentrations where some researchers observed a conductivity minimum? Fig. 1 shows possible explanations. As was discussed by Robertson [16], the band edges of a-C are defined by the π-π^* gap of connected 3-fold sites (i.e. 3-fold clusters) with the gap being inversely proportional to cluster size. Hence, it is possible that at low N concentrations, N promotes the creation of 3-fold coordinated carbon but also stabilizes the 3-fold carbon in small clusters, e.g. closed ring structures such as pyrroles, etc., and inhibits the larger 3-fold chain-like structures. This would lower the conductivity due to an increase in the minimum π-π^* gap. At larger N concentrations, the isolated clusters will merge, creating extended clusters with smaller π-π^* gaps, which is consistent with the observed increases in optical absorption and conductivity. In this way, N acts not as an electronic dopant, but rather as a "microstructural dopant."

The ability to electronically dope a-C(:H) with other dopants is not promising. Meyerson and Smith assumed B acts like a p-type dopant in a-C:H based on their conductivity measurements [3], but Jones and Stewart [5] and Ronning *et al.* [8], who also observed conductivity increases with B incorporation in a-C:H or a-C films, concluded that B was not acting as an electronic dopant. Amaratunga *et al.* did not observe conductivity increases with B incorporation and similarly concluded that B was not acting as a p-type dopant in a-C [11].

1.3 Electrical Transport in a-C

An even more fundamental issue than doping in a-C is the nature of the electronic transport mechanism. Most experimental evidence indicates that electronic transport, particularly near room temperature and at low applied electric fields, behaves according to hopping conduction. The evidence includes: (1) low values for the thermopower [4,6,9], (2) conductivity versus temperature measurements which show deviations from models with a single activation energy [5,7,9,17,18], (3) current-voltage measurements which show ohmic conduction at low fields and Frenkel-Poole emission at high fields [8], and (4) the observed exponential dependence of conductivity on 3-fold content [14].

The specific nature of the hopping conduction is the subject of debate, however. Following Mott and Davis [19], the conductivity, σ, of a system that is determined by nearest neighbor hopping between sites which differ in energy by Δ and are spatially separated by R is given by

$$\sigma = \frac{e^2}{6} R^2 \nu_0 N(E_F) \exp(-2\alpha R - \Delta / k_B T) \ , \qquad (1)$$

where ν_0 is the attempt frequency (typical of phonon frequencies), $N(E_F)$ is the DOS at E_F, and α^{-1} is the localization length. In the disordered system, it is assumed that there will be a distribution of Δ and R, such that the preferred hops may not be nearest neighbor hops, but may be of variable distance away, i.e. "variable range hopping" which is given by Mott and Davis as

$$\sigma = \frac{e^2 \nu_0}{2(8\pi)^{1/2}} \left[\frac{N(E_F)}{\alpha k_B T} \right]^{1/2} \exp\left[-A / T^{-1/4} \right] \ , \qquad (2)$$

with $A \approx 2.1[\alpha^3 / k_B N(E_F)]^{1/4}$. As has been pointed out by several authors, one does not obtain reasonable values for α^{-1} and $N(E_F)$ using the observed conductivities of a-C(:H) – α^{-1} tends to be unphysically small or $N(E_F)$ unphysically large [9,18]. Dasgupta *et al.* suggested one solution to this problem. They assumed that the conductivity in a-C(:H) is determined by hopping not between isolated defect sites but rather between clusters of 3-fold carbon. This gives rise to a form for the conductivity which is very similar to Eq. 1, except R now represents the separation between clusters, assumed to be a few nm [18]. An alternative explanation was suggested by Shimakawa and Miyake [17]. These authors suggested that transport is best described by multiphonon non-polaronic hopping between 3-fold carbon clusters. These authors also concluded that small polaron hopping [20] was not occurring based on their fits to σ vs. T data, although the possibility of polaronic hopping *within* 3-fold carbon clusters cannot

be definitively ruled out. Finally, we present below a third alternative description of electronic transport in a-C films based on combined stress relaxation and electronic transport measurements.

2 Combined Stress Relaxation and Transport Measurements

2.1 Experimental

The a-C films were deposited using pulsed-laser deposition (PLD) with a rotating graphite target and a KrF (248 nm) laser. Films were deposited using high laser fluences, ≥ 50 J/cm^2, to obtain films with high concentrations of 4-fold coordinated carbon, $> \sim 70$ %. For measurements of stress relaxation, the a-C films were deposited on 2" Si(100) wafers to a thickness of ~ 100 nm, and the stress was determined by profilometric measurement of wafer curvature and Stoney's equation [21]. For measurements of electrical transport, the films were deposited to a thickness of ~ 100 nm on TiW-coated Si substrates (200 nm TiW on 1 μm SiO_2 on Si), and Ti-Au metal contacts with areas ranging from 2.5×10^{-5} cm^2 to 1.6×10^{-3} cm^2 were defined on the film surface using photolithography and lift-off. The electrical conductivity through the thickness of the film was determined from the slope of current-voltage scans taken over the range -50 mV to 50 mV, which is in a range in which ohmic behavior is observed [8].

The thermal annealing was performed using a rapid thermal annealer, and identical anneals were performed for both stress relaxation samples and the electrical samples. The time-temperature annealing behavior was determined by performing anneals for successively longer times at each anneal temperature. The measurement of the stress or electrical transport was performed at room temperature, however, and thus any observed changes are due to irreversible processes which have occurred in the material as a result of annealing.

2.2 Stress Relaxation

The time-temperature behavior of stress relaxation in a-C is shown in Fig. 2(a). Surprisingly, complete stress relaxation is observed after annealing a short time at 600°C and noticeable stress relaxation occurs even as low as 100°C. This is a much lower temperature than one would expect for diffusional relaxation processes. We have found that the annealing induces only very minor observable changes in many film properties: negligible changes in EELS, only very slight changes in Raman, and a slight decrease in density (from about 2.95 to 2.85 g/cm^3)

[14,22,23]. There are, however, observable slight increases in optical absorption with annealing and easily identifiable increases in electrical conductivity [14,22].

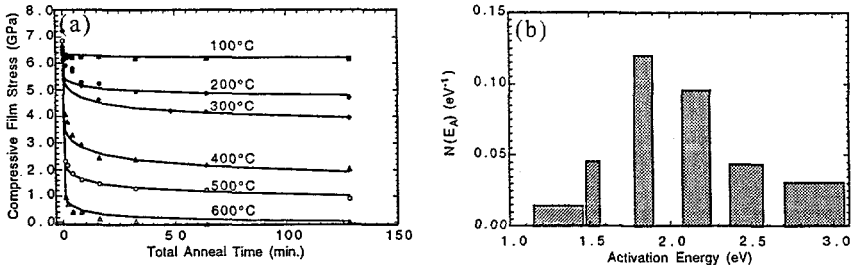

Figure 2: (a) Time– and temperature–dependent stress relaxation in a-C. Solid lines are fits to the data using the stress relaxation model. (b) Derived distribution in activation energy, $N(E_A)$, for conversion of 4-fold coordinated carbon to 3-fold coordinated carbon.

A model has been developed to explain the unique stress relaxation in this material [14]. The model assumes that thermal annealing causes some 4-fold coordinated carbon atoms in a-C to convert to 3-fold coordinated carbon atoms by a process which is thermodynamically favored but kinetically limited. The biaxial stress state of the film causes the strain energy for the 4-fold to 3-fold conversion to be unfavorable unless the newly created 3-fold sites are oriented such that the sp^2 bonds are in the plane of the film. When this occurs, the film accommodates the biaxial compressive stress by contracting in the plane of the film and expanding in the direction normal to the film. The net result is a decrease in film stress and a slight increase in the concentration of 3-fold coordinated carbon atoms (which gives rise to a density decrease, increase in optical absorption, and an increase in electrical conductivity). The model time-temperature stress relaxation response is given by

$$\sigma(t,T) = \sigma_0 + \frac{\varepsilon_{sp^2-sp^3} E}{1-\nu} \int_0^\infty N(E_A)\left\{1 - \exp\left[-\nu_0 t \exp\left(-E_A / k_B T\right)\right]\right\} dE_A \ , \qquad (3)$$

where $\sigma(t,T)$ is the time and temperature-dependent stress, σ_0 is the initial in-plane stress, E is the elastic modulus of a-C, ~ 1000 GPa, ν is the Poisson ratio, which we assume to be 0.3, $\varepsilon_{sp^2-sp^3}$ is the strain associated with replacing a 4-fold atom with a 3-fold atom (~ –0.08), ν_0 is the attempt frequency (about 10^{13} sec^{-1}), and $N(E_A)dE_A$ is the fraction of 3-fold sites which are converted from 4-fold sites with an activation energy in the range dE_A.

By fitting the stress relaxation data using Eq. 3 [see the solid lines in Fig. 2(a)], we obtain the distribution of $N(E_A)$, the distribution of activation energies for converting 4-fold carbon to 3-fold carbon. This distribution is shown in Fig. 2(b). The activation energy for transformation begins around 1 eV, but most sites have an activation energy of 2 eV or higher. This should be compared to the activation energy of 0.7 eV for conversion of sp^3 bonds to sp^2 bonds at defect sites in crystalline diamond that was found by Reznik *et al.* by looking at changes in hopping site density [24]. This 0.7 eV activation energy is near the onset activation energy we observe in Fig. 2(b) and is consistent with our observations that stress relaxation is already noticeable at temperatures of 100°C.

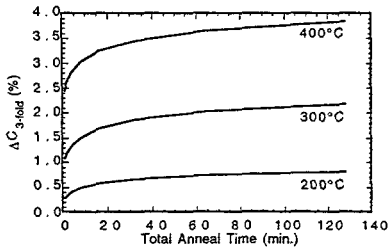

Figure 3: Change in 3-fold carbon concentration with time and temperature as derived from the stress relaxation model.

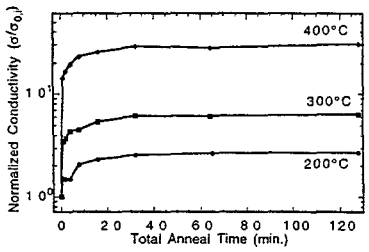

Figure 4: Conductivity of a-tC measured at room temperature following time-temperature annealing.

From the distribution of $N(E_A)$, Fig. 2(b), we may determine the change in 3-fold coordinated carbon concentration, ΔC_{3-fold}, as a function of time and temperature. For full stress relaxation, it is only necessary that the 3-fold concentration in the sample increase by 6.5 at. %, i.e. from an initial value of 30% to a final value of 36.5%. The majority of the sample is still 4-fold coordinated, which explains why the material exhibits little observable change in Raman, EELS, or hardness [23]. At lower temperatures, fewer additional 3-fold sites are created. Fig. 3 shows the change in 3-fold concentration with time and temperature for annealing temperatures between 200 and 400 °C as derived from Fig. 2(b).

2.3 Electrical Measurements

The change in conductivity of a-C films as a function of time-temperature annealing is shown in Fig. 4. The initial conductivity measured at different sites (i.e.

different contacts) on the same sample shows large variation, so the conductivity curves are normalized by the initial conductivity, $\sigma_{0,i}$, for the particular site measured [14]. Typical conductivities prior to annealing were 10^7 Ωcm. By combining the data in Fig. 4 with the derived changes in 3-fold concentration, Fig. 3, we obtain the dependence of conductivity on the change in 3-fold concentration which is shown in Fig. 5. The temperatures indicated on the plot are the anneal temperatures at which the data was taken.

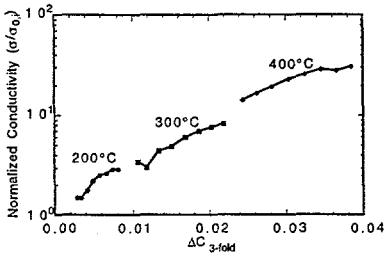

Figure 5: Plot showing the combined electrical conductivity and change in 3-fold concentration. The 3-fold concentration was determined from the distribution in activation energies.

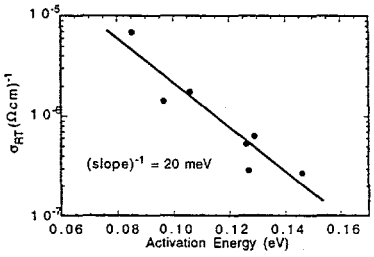

Figure 6: The activation energy for current transport measured at several sites on the same sample. In good approximation, the variation in conductivities is due to variation in activation energies.

The data in Fig. 5 reveals that there is an exponential dependence of the normalized conductivity to the change in 3-fold carbon concentration, $\sigma = \sigma_{0,i} \exp(\kappa \Delta C_{3-fold})$, where $\kappa \approx 100$. The "activation energy" for conduction was also measured at several sites by varying the temperature of the conductivity measurement between 220 K and 380 K. This temperature range is not sufficient to reliably distinguish the exponent α in the conductivity expression $\sigma = \sigma_0 \exp(-A / T^{\alpha})$, so $\alpha = 1$ was assumed, implying $E_A = A/k_B$. As is shown in Fig. 6, the variation in conductivity is primarily due to changes in the activation energy (or the factor 'A' for non-unity α).

2.4 Discussion

As has already been pointed out by others, the conductivity of a-C films is not accurately described by classical variable range hopping of Mott and Davis, Eq. 2 [9,18]. One solution was suggested by Dasgupta *et al.* [18]. These authors

assumed that variable range hopping does not occur between isolated 3-fold sites, but rather nearest neighbor hopping between three-dimensional clusters of 3-fold sites occurs. A problem with this model is that the suggested nearest neighbor hopping distance, about 3 nm, would imply that the 3-fold clusters should be visible by high resolution transmission electron microscopy (HRTEM), which is not observed. Recently, several theoretical works have indicated that the 3-fold sites do not tend to form 3-D clusters, but rather they tend to form extended chain-like structures with fractal dimension between 1 and 2 [2]. The presence of chain-like structures for the 3-fold sites is still consistent with the observed optical absorption properties of a-C [16], but, more importantly, it is more consistent with the observed electrical properties.

For the system consisting of various size 3-fold "chains" in a matrix of 4-fold sites, the conduction problem can be solved by treating the system as a random resistor network and considering all possible current pathways. We are currently working on this general problem, but the qualitative features of the model can be readily extracted. The local DOS of the 3-fold carbon chains is dominated by the π-π^* gap, which is a function of chain length (i.e. the number of carbon atoms in the chain). As was pointed out by Robertson, the π-π^* gap, $E_{\pi-\pi^*}$, of conjugated chains varies as ~ 20 eV/N, where N is the number of carbon atoms in the chain (this gap should be slightly reduced for chains embedded in a solid) [16]. If we assume the carriers are thermally activated into the π or π^* states of the chain, then $E_A \sim 1/2\, E_{\pi-\pi^*} \approx 10$ eV / N. (It is also possible that electron propagation along the chain obeys polaronic hopping, in which case the polaron energy, W, would have a different, as yet unknown, dependence on N.) Taking the view of thermal activation into π or π^* states, it is clear that in a conductivity measurement, carriers will be preferentially promoted to the π or π^* states of the longest chains. In order for the carriers to propagate through the solid, they must tunnel to another chain, but not just to any neighboring chain. Tunneling into the π and π^* states of shorter chains is not possible because of lack of overlap between initial and final states ($E_{\pi-\pi^*}$ of the small chains is larger than $E_{\pi-\pi^*}$ of the long chains). Therefore, it is necessary to tunnel into another chain of similar length or larger (similar length between defined as chains with similar $E_{\pi-\pi^*} \pm k_B T$). Not just any long chain will work, however, since it is also necessary to ensure overlap in the π orbitals between chains, and this requires that the π orbitals be similarly oriented. This is an important effect as it has been shown that disorder in the π orbital orientation is one of the primary reasons for the strong localization in a-C [25]. The conductivity in a-C can, therefore, best be described as both variable range hopping and "variable orientation" hopping because both the separation between

long chains and relative orientation of the π orbitals in the chains are important. Because transport is dominated by those few favored conduction paths, considerable variation in conductivity from site to site is to be expected and is observed [14].

We can obtain a qualitative estimate for a typical length of a 3-fold carbon chain responsible for conductivity in a-C. If we assume that the effect of thermal annealing leads to chain ripening such that a chain of N carbon atoms grows to a chain of N+ΔN, then

$$E_A = \frac{\beta'}{N+\Delta N} \approx \frac{\beta'}{N}\left(1-\frac{\Delta N}{N}\right), \tag{4}$$

where the dependence of $E_{\pi-\pi^*}$ on N is contained within β'. From Fig. 6, we obtain $\sigma = \sigma_0 \exp(-E_A / k_B T)$, so

$$\sigma = \sigma_0 \exp(-\beta' / N k_B T) \exp[(\beta' / N)(\Delta N / N)(1 / k_B T)] . \tag{5}$$

From Fig. 5, $\sigma = \sigma_{0,i} \exp(\kappa \Delta C_{3-fold})$, where $\sigma_{0,i} = \sigma_0 \exp(-\beta' / N k_B T)$. Equating gives

$$\left(\frac{\beta'}{N}\right)\left(\frac{\Delta N}{N}\right)\frac{1}{k_B T} = \kappa \Delta C_{3-fold} = \kappa C_0 \left(\frac{\Delta N}{N}\right), \tag{6}$$

where C_0 is the initial 3-fold carbon concentration. Solving for N, we obtain that

$$N = \frac{\beta'}{\kappa C_0 k_B T} . \tag{7}$$

Assuming β' = 10 eV, C_0 = 0.3, κ = 100 (from Fig. 5), and $k_B T$ = 0.025 eV (the measurement temperature in Fig. 5 was room temperature), we obtain N=13. This value of N is physically reasonable and is still consistent with the fact that clusters of 3-fold sites are not observed in HRTEM. Thermal annealing at 400°C only increases N from 13 to ~ 14, but this is sufficient to explain the factor of 35 increase in conductivity which is observed. The value of N obtained should not be taken too seriously as the fractal dimension of the "chains" and the true dependence of $E_{\pi-\pi^*}$ on N are not presently known.

The heterogeneous conduction process implied by chain-to-chain tunneling in a-C has interesting implications. One implication is that it may help explain why electron field emission from a-C tends to be spatially localized [26]. Consider the following emission model: (1) Because of heterogeneous conduction, there may be some regions of the sample in which a conduction path in the a-C film does not quite reach the film surface. We assume that between the surface and the conduction

path is a region of predominantly 4-fold carbon which acts as a tunnel barrier (thickness ~ 5 nm or less). (2) An electron from a π^* state in the conductive path beneath the tunnel barrier must Fowler-Nordheim tunnel through the barrier layer to reach vacuum, but this process is unlikely except for very high fields. If, instead, positively-charged traps are located within the tunnel barrier, then a dipole layer is established which permits ready Fowler-Nordheim emission into vacuum, see Fig. 7 (we note that in an emission model for a-C:N films, positively charged defects were assumed to be present in the bulk of the film [27]). (3) If the positively-charged traps recombine with an electron and become neutral, the emission site switches off until the traps can again become field ionized. This might explain the switching on and off of emission sites which is frequently observed and described as "twinkling". The emission model described here is, as yet, untested, but it does explain why the emission sites are localized, why the turn-on field and apparent work function for a-C are anomalously low, why the emission sites show twinkling, why the emission sites in a-C seem unaffected by surface contamination, and why the emitted electrons appear to originate near E_F [28].

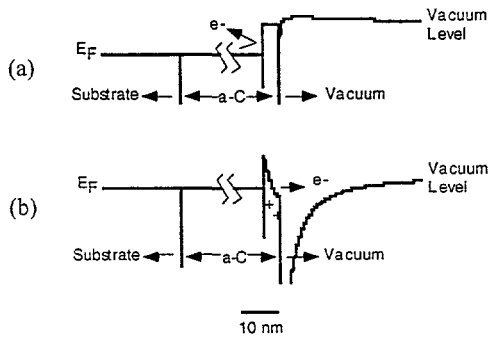

Figure 7: Tunnel barrier emission model. (a) Thin, 5 nm thick uncharged tunnel barrier at the surface of the a-C film. (b) Tunnel barrier containing positively charged trap states. An applied field of 10 V/μm, a positively charged trap state density of 4 x 10^{18} cm^{-3}, a CB to E_F offset of 2 eV, an electron affinity (of the tunnel barrier region) of 0.5 eV, a work function (of the non-tunnel barrier region) of 2.5 eV, and a tunnel barrier with the geometry of a disk 5 nm in width and 100 nm in radius were assumed.

3 Conclusions and Acknowledgments

Electronic transport mechanisms in a-C films and doping have been the subject of much debate, but at least at low fields and near room temperature or below, the conductivity obeys hopping transport. Combined stress relaxation and electrical transport studies were used in this study to identify the transport mechanism in a-C

films prepared by pulsed-laser deposition. It was observed that the conductivity of a-C films is exponentially proportional to increases in carbon 3-fold concentration. This result is consistent with thermally activated hopping along carbon 3-fold chains combined with chain-to-chain tunneling. From the data, a typical chain length contributing to the conductivity was estimated to consist of 13 carbon atoms. The heterogeneous nature of the conductivity may explain the spatially localized electron emission which is observed in a-C assuming a tunnel barrier emission model.

Support, discussions, or experimental assistance from R. G. Dunn, J. Mikkalson, N. Missert, M. P. Siegal, E. B. Stechel, E. L. Venturini, and Motorola Corp. are gratefully acknowledged. Sandia is a multiprogram laboratory operated by Sandia Corp., a Lockheed Martin Co., for the U.S. Dept. of Energy under Contract DE-AC04-94AL85000.

References

1. J. E. Jaskie, MRS Bull. **21**, 59 (1996).
2. see, for example, Th. Frauenheim, G. Jungnickel, Th. Köhler, P. Stitch, and P. Blaudeck, this volume; N. A. Marks, D. R. McKenzie, B. A. Pailthorpe, M. Bernasconi, and M. Parrinello, Phys. Rev. Lett. **76**, 768 (1996); P. A. Schultz and E. B. Stechel, to appear in Phys. Rev. B.
3. B. Meyerson and F. W. Smith, Solid State Commun. **34**, 531 (1980).
4. B. Meyerson and F. W. Smith, Solid State Commun. **41**, 23 (1982).
5. D. I. Jones and A. D. Stewart, Phil. Mag. B **46**, 423 (1982).
6. O. Amir and R. Kalish, J. Appl. Phys. **70**, 4958 (1991); R. Kalish, O. Amir, R. Brener, R. A. Spits, and T. E. Derry, Appl. Phys. A 52, **48** (1991).
7. O. Stenzel, M. Vogel, S. Ponitz, R. Petrich, T. Wallendorf, C. V. Borczyskowski, F. Rozploch, Z. Krasilnik, and N. Kalugin, Phys. Stat. Sol. A **140**, 179 (1993).
8. C. Ronning, U. Griesmeier, M. Gross, H. C. Hofsäss, R. G. Downing, and G. P. Lamaze, Diamond Relat. Mater. **4**, 666 (1995).
9. A. Helmbold, P. Hammer, J. U. Thiele, K. Rohwer, and D. Meissner, Phil. Mag. B **72**, 335 (1995).
10. V. S. Veerasamy, J. Yuan, G. A. J. Amaratunga, W. I. Milne, K. W. R. Gilkes, M. Weiler, and L. M. Brown, Phys. Rev. B **48**, 17954 (1993); V. S. Veerasamy, G. A. J. Amaratunga, C. A. Davis, A. E. Timbs, W. I. Milne, and D. R. McKenzie, J. Phys. Cond. Mater. **5**, L169 (1993); V. S.

Veerasamy, G. A. J. Amaratunga, J. S. Park, H. S. McKenzie, and W. I. Milne, IEEE Trans. Electron. Dev. **42**, 577 (1995).
11. G. A. J. Amaratunga, V. S. Veerasamy, C. A. Davis, W. I. Milne, D. R. McKenzie, J. Yuan, and M. Weiler, J. Non-Cryst. Solids **164-166**, 1119 (1993).
12. S. R. P. Silva, B. Rafferty, G. A. J. Amaratunga, J. Schwan, D. F. Franceschini, and L. M. Brown, Diamond Relat. Mater. **5**, 401 (1996); S. R. P. Silva, J. Robertson, G. A. J. Amaratunga, B. Rafferty, L. M. Brown, J. Schwan, D. F. Franceschini, and G. Mariotto, J. Appl. Phys. **81**, 2626 (1997).
13. A. Mansour and D. Ugolini, Phys. Rev. B **47**, 10201 (1993).
14. J. P. Sullivan, T. A. Friedmann, and A. G. Baca, J. Electron. Mater. **26**, 1021 (1997).
15. S. R. Elliot, *Physics of Amorphous Materials, 2nd Ed.* (John Wiley & Sons, New York, 1990).
16. J. Robertson, Adv. Phys. **35**, 317 (1986).
17. K. Shimakawa and K. Miyake, Phys. Rev. Lett. **61**, 7584 (1988); K. Shimakawa and K. Miyake, Phys. Rev. B **39**, 7578 (1989).
18. D. Dasgupta, F. Demichelis, and A. Tagliaferro, Phil. Mag. B **63**, 1255 (1991).
19. N. F. Mott and E. A. Davis, *Electronic Processes in Non-Crystalline Materials, 2nd Ed.* (Oxford University Press, Oxford, UK, 1979).
20. D. Emin, Adv. Phys. **24**, 305 (1975); E. Gorham-Bergeron and D. Emin, Phys. Rev. B **15**, 3667 (1977).
21. G. G. Stoney, Proc. R. Soc. London, Ser. A **82**, 172 (1909).
22. J. P. Sullivan, T. A. Friedmann, D. R. Tallant, J. Mikkalson, D. Rieger, A. G. Baca, and L. J. Martiñez-Miranda, to be published.
23. T. A. Friedmann, J. A. Knapp, D. L. Medlin, P. B. Mirkarimi, J. P. Sullivan, D. R. Tallant, R. L. Simpson, and J. Mikkalson, to be published.
24. A. Reznik, V. Richter, and R. Kalish, Phys. Rev. B **56**, 7930 (1997).
25. J. Robertson, Phil. Mag. B **76**, 335 (1997).
26. N. Missert, T. A. Friedmann, J. P. Sullivan, and R. G. Copeland, Appl. Phys. Lett. **70**, 1995 (1997).
27. G. A. J. Amaratunga and S. R. P. Silva, Appl. Phys. Lett. **68**, 2529 (1996).
28. O. Gröning, O. M. Küttel, P. Gröning, and L. Schlapbach, Appl. Phys. Lett. **71**, 2253 (1997).